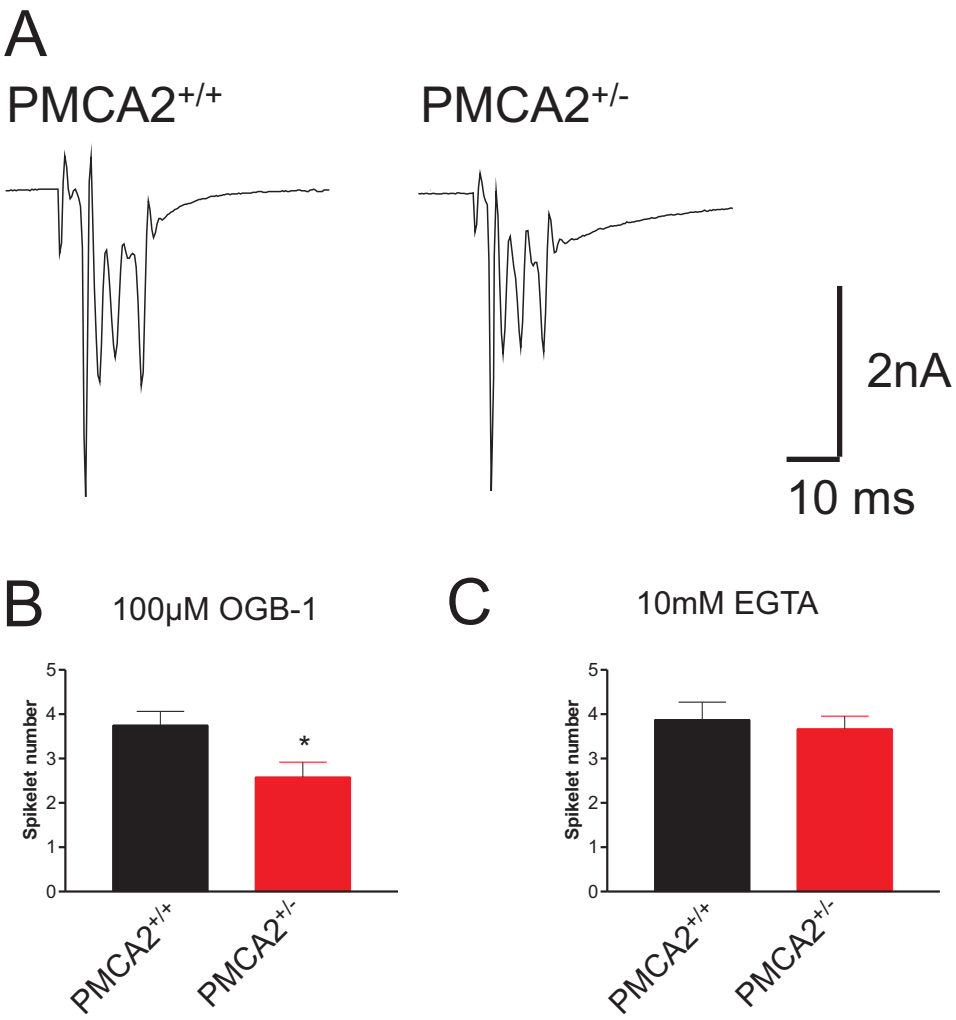

Supplementary Figure 1. High levels of the exogenous calcium buffer EGTA rescued the climbing fibre responses in PMCA2$^{+/-}$ Purkinje neurones.

A shows representative traces from climbing fibre evoked inward current responses from PNs recorded with an intracellular whole-cell patch solution containing 10 mM EGTA. Climbing fibre responses were similar between wild type, PMCA2$^{+/+}$ and PMCA2$^{+/-}$ cells as seen by the similar number of repetitive spikelets; this was the case in both voltage clamp and current clamp. These results contrasted to the result shown in the main Figure 2 where the climbing fibre electrophysiological response was weaker in the PMCA2$^{+/-}$ PNs when the responses were recorded with minimal calcium buffering offered by 100 μM Oregon Green BAPTA-1 (OGB-1).

The combined data for all cells is shown in *B* and *C*. In B the mean number of spikelets in PMCA2$^{+/-}$ cells was reduced when intracellular calcium buffering was minimal but restored to control levels when intracellular calcium was heavily buffered by 10 mM EGTA. *represents a significance level at $p<0.05$ t-test.

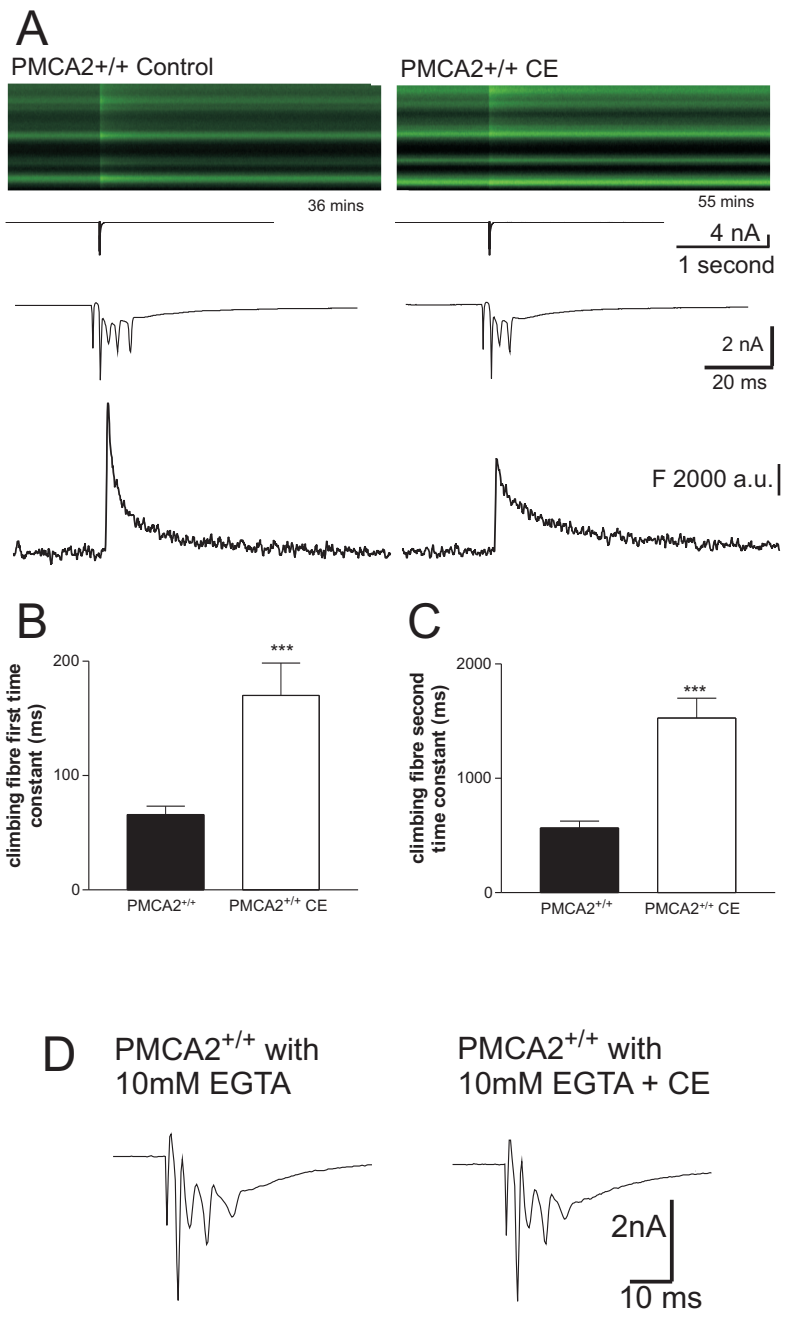

Supplementary Figure 2. Climbing fibre calcium transients were slowed and the number of spikelets reduced following application of the PMCA inhibitor carboxyeosin, CE.

A shows x-t plots of fluorescence from a set of dendrites from a representative PMCA2$^{+/+}$ wild type Purkinje neurone before and after the application of 10 µM carboxyeosin, CE. The left hand plot was recorded 36 minutes after the whole cell patch clamp configuration was established and just before the application of carboxyeosin; the right hand x-t plot was recorded in the presence of carboxyeosin from the same set of dendrites approximately 19 minutes later. Directly below the x-t plot is the simultaneously obtained electrophysiological response at slow time resolution and below this is the higher time resolved climbing fibre response showing the first sodium dependent inward current followed by the repetitive spikelets. Carboxyeosin application reduced the number of spikelets, as seen in this cell, whilst also reducing the amplitude, and slowing the recovery of both fast and slow phases of the climbing fibre induced calcium transient, fluorescence trace below.

B and *C* show the combined data for the fast and slow time constants respectively from all cells before and after the application of carboxyeosin, filled versus open bars. In *D* a representative cell shows that climbing fibre responses from 10mM EGTA-filled wild type PCMA2$^{+/+}$ cells were unaffected by carboxyeosin, mean values are quoted in the main results.

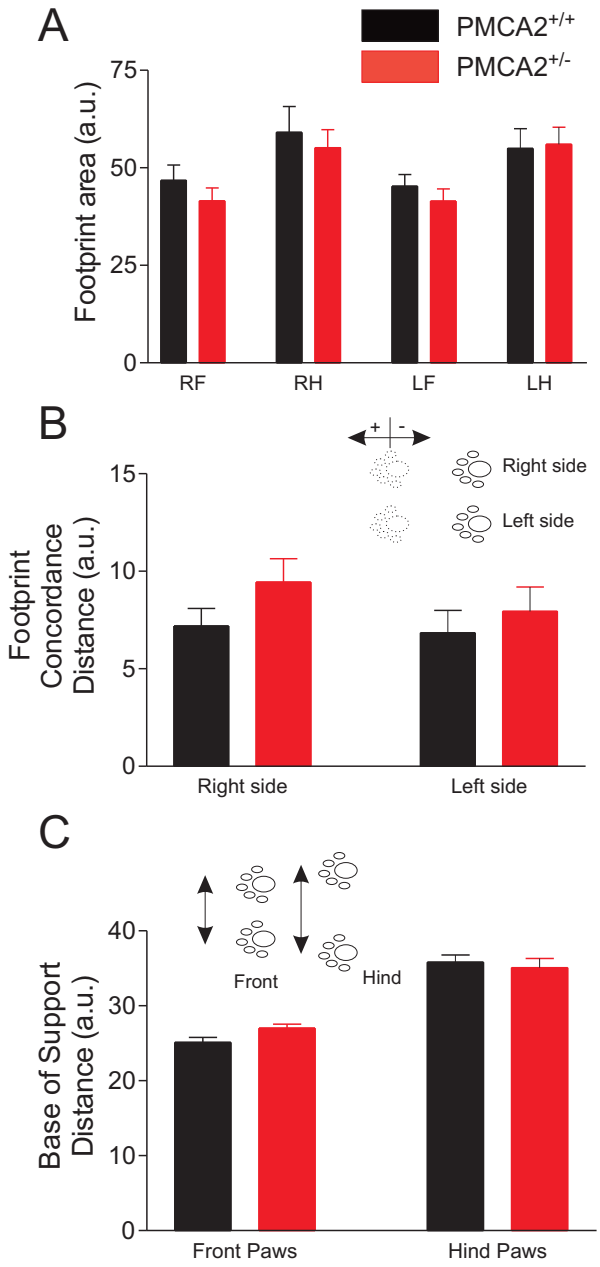

Supplementary Figure 3. Gait parameters as assessed by Catwalk are normal in PMCA2$^{+/-}$ mice.
Analysis used footprint parameters extracted from 3-5 consecutive trials of age-matched litter mate PMCA2$^{+/+}$ mice, n=8 and PMCA2$^{+/-}$ mice, n=13, from three separate litters. Variance of all parameters followed a normal distribution and allowed mean values for all trials from each mouse to be pooled and then compared with two way ANOVA.
In *A*, footprint area is unchanged between wild type PMCA2$^{+/+}$ mice (black bars) and PMCA2$^{+/-}$ mice (red bars). Two way ANOVA revealed no significant effect of genotype but a significant difference between the front and hind paw areas of contact, p=0.35 and p<0.001 respectively. This indicates that the mice apply more body weight to their hind paws and that this is similar between the groups. Area values are in pixels.
B shows footprint concordance results from measurements made from both sides of the mouse. As shown in the inset, concordance measures how closely the hind footprint overlaps with the front footprint (dotted print). If the hind print arrives in front of the position that the fore print had previously occupied then a positive value is recorded, +, if however the hind print lags behind the foreprint then a negative value is recorded. We noted considerable variation between prints within mice, both + and - values being collected from both PMCA2$^{+/+}$ and PMCA2$^{+/-}$ mice. As shown in the Figure both PMCA2$^{+/+}$ and PMCA2$^{+/-}$ mice showed significant discordance from zero, with a clear tendency for their left and right hind paws to arrive in front of their previous foreprint position, with values around +5 pixels. Two way ANOVA did not detect any significant differences; right and left sides were similar (as expected), p=0.49, and there was no effect of genotype, p=0.21, although as can be seen by comparing the red (PMCA2$^{+/-}$) and black (PMCA2$^{+/+}$) bars there was a tendency towards a greater concordance on both sides in the PMCA2$^{+/-}$ mice. A similar, but significant, finding has been observed in another mouse model of ataxia where there was little evidence of degeneration (Shattokai et al. 2004, J Clin Invest. 113(4):582-90).
In *C* the combined base of support measurements from the distance between the front and hind paws, as depicted in the inset, are shown. Two way ANOVA revealed a significant difference between front and rear measurements p<0.0001, but no significant effect of genotype, p=0.56, black PMCA2$^{+/+}$ and PMCA2$^{+/-}$ bars respectively.